ITM-09-IMP5-T3: FAST ICRH CODE FOR ROUTINE ANALYSIS
VR:T. Hellsten, A. Hannan, T. Johnson, J. Höök

ITM – 2011-ACT4 Synergetic Effects between NBI and ICRH

ITM-09-IMP5-T5: DEVELOPMENT OF AN ADVANCED 3D FOKKER –PLANCK SOLVER FOR IONS FOR ORBIT AVERAGED MONTE CARLO CODE.
VR: T. Hellsten, Q. Mukhtar, T. Johnson, J. Höök.

ITM-09-IMP5-T5: ADOPTIVE δf-METHOD FOR ICRH
VR: J. Höök, T. Hellsten

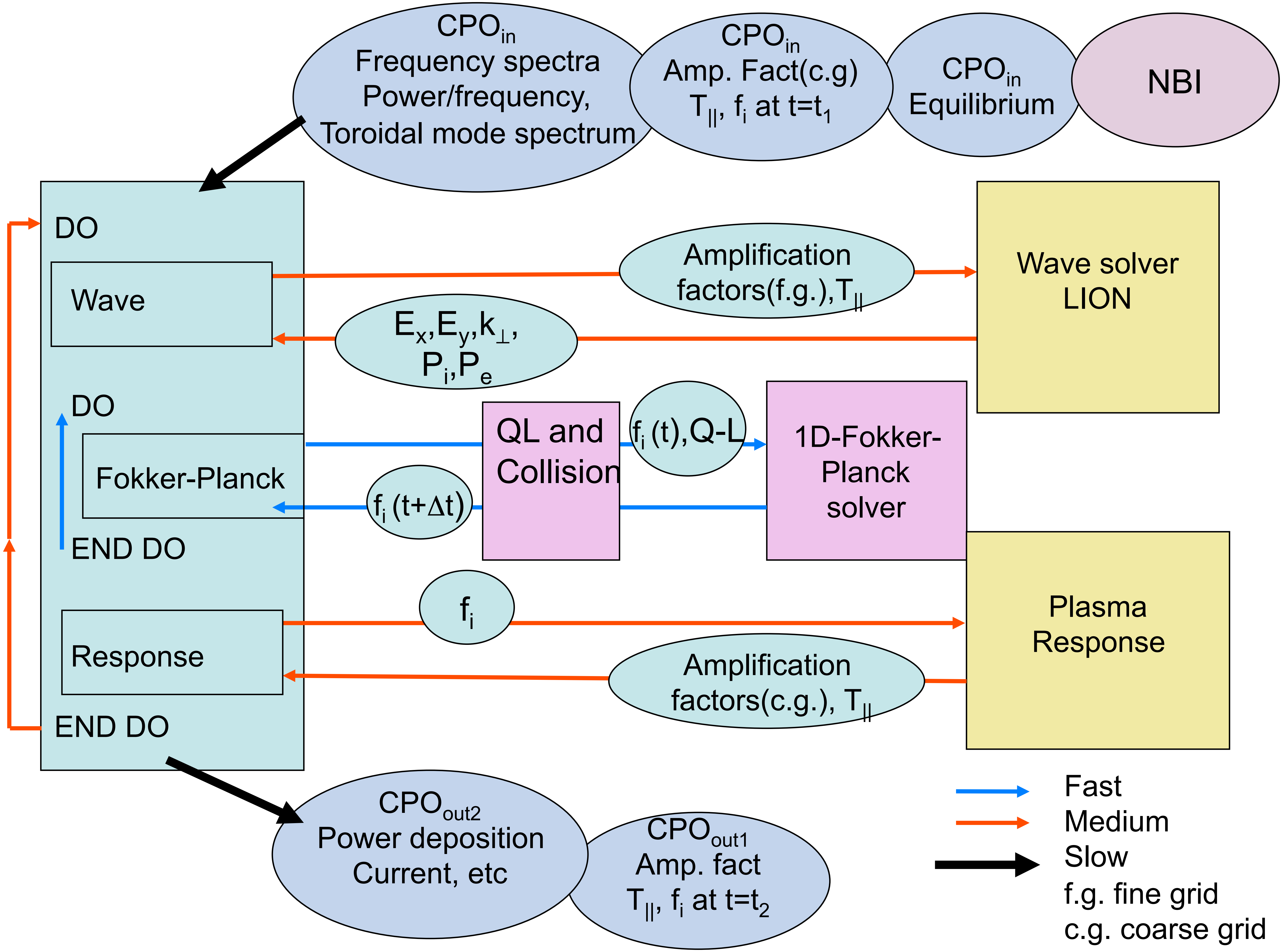
CPO$_{in}$
Frequency spectra
Power/frequency,
Toroidal mode spectrum
CPO$_{in}$
Amp. Fact(c.g)
$T_{||}$, f_i at $t=t_1$
CPO$_{in}$
Equilibrium
NBI
DO
Wave
Amplification factors(f.g.),$T_{||}$
Wave solver LION
E_x,E_y,$k_\perp$, P_i,P_e
DO
Fokker-Planck
END DO
QL and Collision
f_i (t),Q-L
1D-Fokker-Planck solver
f_i (t+Δt)
f_i
Plasma Response
Response
Amplification factors(c.g.), $T_{||}$
END DO
CPO$_{out2}$
Power deposition
Current, etc
CPO$_{out1}$
Amp. fact
$T_{||}$, f_i at $t=t_2$
Fast
Medium
Slow
f.g. fine grid
c.g. coarse grid

ITM-09-IMP5-T3: Fast ICRH code for routine simulation IMP-3

- The global code LION used for wave field calculations
- A time dependent cubic FEM code for the pitch angle averaged distribution functions
- The quasi-linear RF-operators in the Fokker-Planck code are calculated by averaging the wave field and quantities obtained from the wave solver over a nested set of subvolumes
- A benchmarked formula is used to calculate a parallel temperature from the pitch angle averaged distribution function
- The susceptibility tensors of the resonant ion species are modified by flux surface averaged amplification factors as the distribution functions evolves
- Four time scales, $t_1 > t_2 > t_3 > t_4$, are used to achieve that the coupled power by each toroidal mode agrees with the absorbed power
- Source terms for modelling NBI and fusion reaction product or a local Maxellian to allow modelling of the changes of the resonant ion densities either to agree with measurements or transport modelling
- Poloidal wave number important for damping by TTMP and tail formation

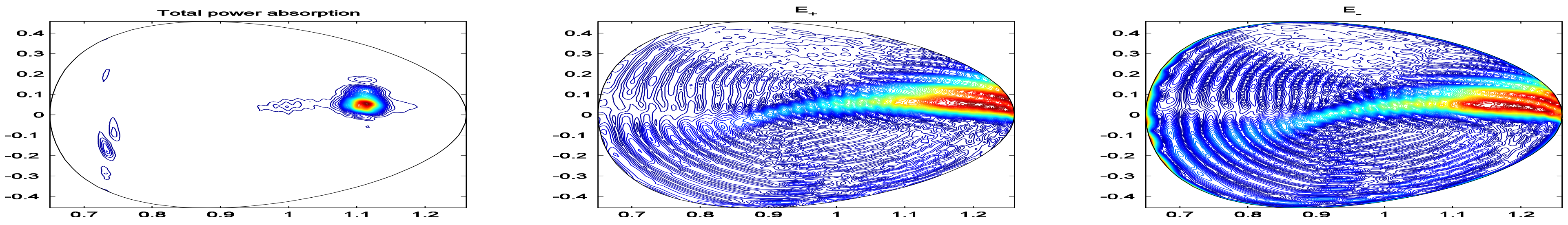

Power deposition and wave field for strong single pass damping

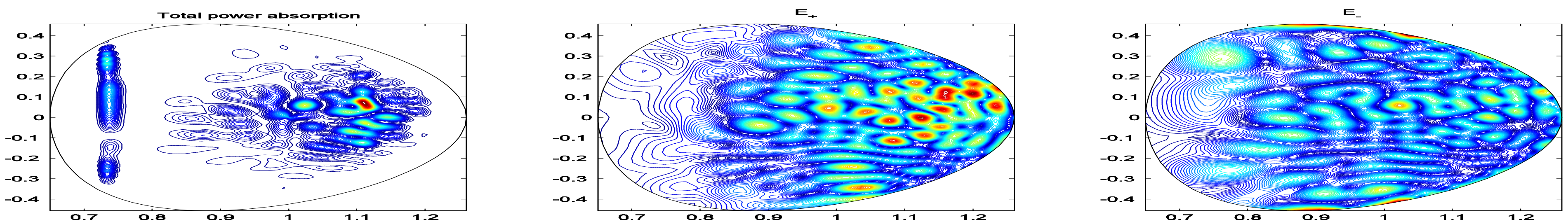

Power deposition and wave field for weak single pass damping

Fast ICRH code for routine simulation IMP-3

Different models of the Fokker-Planck coefficients and susceptibility tensor are used for weak and strong single pass damping.

$$\frac{\partial F_n}{\partial t} = \frac{\partial}{\partial \upsilon}\left[-\alpha F_n + \frac{1}{2}\frac{\partial}{\partial \upsilon}\left(\beta F_n\right)\right] + \frac{\partial}{\partial \upsilon}\left[H_l\left(\frac{k_\perp \upsilon}{\omega_{ci}}\right)\left(\frac{\partial F_n}{\partial \upsilon} - \frac{2F_n}{\upsilon}\right)\right] + S_n(\upsilon)$$

where $$H_l\left(\frac{k_\perp \upsilon}{\omega_{ci}}\right) = \left|E_+ J_{l-1} + e^{-2i\zeta} E_- J_{l+1}\right|^2 = \left|\bar{E}_+ J_{l-1}\right|^2 + \left|\bar{E}_- J_{l+1}\right|^2 + 2\tau\left|\bar{E}_+^* \bar{E}_-\right| J_{l-1} J_{l+1}$$

Modifications of the susceptibility tensors $$a_{ik}^{(n,l)} = \frac{\chi_{ik}^{(n,l)}\left(f_n\right)}{\chi_{ik}^{(n,l)}\left(f_{M,n}\right)}$$

$$\chi_{ij}^{(nl)}\left(f_n\right) \approx \frac{\omega_p^2}{8\omega\omega_c}\int_0^\infty d_{ij}^{(nl)} \frac{\partial f_n}{\partial \upsilon} \upsilon^2 d\upsilon$$

$$d_{\psi\psi}^{(n,l)} \approx 0.25\left|J_{l-1}^2 + J_{l+1}^2 + 2\tau J_{l-1} J_{l+1}\right| \qquad d_{\chi\chi}^{(n,l)} \approx 0.25\left|J_{l-1}^2 + J_{l+1}^2 - 2\tau J_{l-1} J_{l+1}\right|$$

$$d_{\psi\chi}^{(n,l)} \approx i0.25\left(J_{l-1}^2 - J_{l+1}^2\right)$$

Models are using $\tau = 1$ for strong single pass and $\tau = 0$ for weak.

Fast ICRH code for routine simulation IMP-3

Improved model for calculating the electron damping due to TTMP/ELD in the LION code.
When comparing LION with AORSA LION had slightly higher electron damping and lower second harmonic damping. FWCD was higher.

Previously the electron damping was calculated from a local homogeneous dispersion relation assuming plane waves using $-\omega B_{||} = k_{\xi} E_{\chi}$

After solving the wave field we correct the electron damping by calculating the magnetic fluctuation of the wave field. $-i\omega B_{||} = \mathbf{B}_0 \cdot \nabla \times \mathbf{E}$

This reduce the electron absorption, in particular near the centre.

Fast ICRH code for routine simulation IMP-3

Code verifications and validation.

Verifications of the LION code for electron damping.

Verifications of SELFO-light with PION.

Validation of SELFO-light with DIII higher harmonic FWCD.

Including NBI

Validation of SELFO-light with DIII higher harmonic FWCD with NBI

Fast ICRH code for routine simulation IMP-3

Validation of SELFO-light with DIII higher harmonic FWCD.
The power partition for higher harmonic damping is sensitive to distribution functions and thus power.
Good test case for testing the dynamics of the self-consistent modelling.

Typically power to ions for third harmonic D starts from 14% increases up to 45%.

Currents are in good agreements with experiments in absence of beams problem with runaway because losses not introduced.

ITM-09-IMP5-T5: Alogorithms for δf-method Monte Carlo Methods for ICRH

VR: J. Höök, T. Hellsten,

This δf-method requires new source particles with +/- weights.

Resampling is required. In multi dimensional Monte carlo methods one does not want to project the solution on FEM basis.

A method has been developed to resample by finding neighbouring particles and combining them to fewer particles.

VR: Q. Mukhtar, T. Hellsten, T. Johnson

ITM-09-IMP5-T5

Test model operator in 2D radius and pitch angle

Develop 2D Monte Carlo operators that relaxes the density of the resonant species to given profiles e.g. given by a transport solver.

Convergence error on near magnetic axis.

Using reflection at boundaries instead of reducing time steps.